

Photosynthetic Water Oxidation: Insights from Manganese Model Chemistry

Karin J. Young,[†] Bradley J. Brennan, Ranitendranath Tagore,[‡] and Gary W. Brudvig*

Yale Energy Sciences Institute and Department of Chemistry, Yale University, New Haven, Connecticut 06520-8107, United States

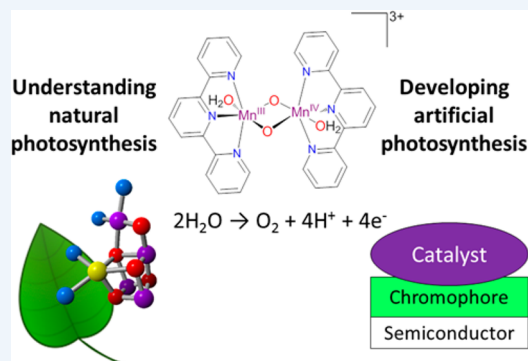
CONSPECTUS: Catalysts for light-driven water oxidation are a critical component for development of solar fuels technology. The multielectron redox chemistry required for this process has been successfully deployed on a global scale in natural photosynthesis by green plants and cyanobacteria using photosystem II (PSII). PSII employs a conserved, cuboidal Mn_4CaO_x cluster called the O_2 -evolving complex (OEC) that offers inspiration for artificial O_2 -evolution catalysts.

In this Account, we describe our work on manganese model chemistry relevant to PSII, particularly the functional model $[Mn^{III/IV}_2(terpy)_2(\mu-O)_2(OH_2)_2](NO_3)_3$ complex (terpy = 2,2',6',2''-terpyridine), a mixed-valent di- μ -oxo Mn dimer with two terminal aqua ligands. In the presence of oxo-donor oxidants such as HSO_5^- , this complex evolves O_2 by two pathways, one of which incorporates solvent water in an O–O bond-forming reaction. Deactivation pathways of this catalyst include comproportionation to form an inactive $Mn^{IV}Mn^{IV}$ dimer and also degradation to MnO_2 , a consequence of ligand loss when the oxidation state of the complex is reduced to labile Mn^{II} upon release of O_2 . The catalyst's versatility has been shown by its continued catalytic activity after direct binding to the semiconductor titanium dioxide. In addition, after binding to the surface of TiO_2 via a chromophoric linker, the catalyst can be oxidized by a photoinduced electron-transfer mechanism, mimicking the natural PSII process.

Model oxomanganese complexes have also aided in interpreting biophysical and computational studies on PSII. In particular, the μ -oxo exchange rates of the Mn–terpy dimer have been instrumental in establishing that the time scale for μ -oxo exchange of high-valent oxomanganese complexes with terminal water ligands is slower than O_2 evolution in the natural photosynthetic system. Furthermore, computational studies on the Mn–terpy dimer and the OEC point to similar Mn^{IV} –oxyl intermediates in the O–O bond-forming mechanism.

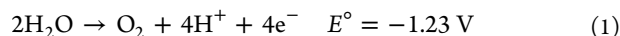
Comparison between the OEC and the Mn–terpy dimer indicates that challenges remain in the development of synthetic Mn water-oxidation catalysts. These include redox leveling to couple multielectron reactions with one-electron steps, avoiding labile Mn^{II} species during the catalytic cycle, and protecting the catalyst active site from undesired side reactions.

As the first example of a functional manganese O_2 -evolution catalyst, the Mn–terpy dimer exemplifies the interrelatedness of biomimetic chemistry with biophysical studies. The design of functional model complexes enriches the study of the natural photosynthetic system, while biology continues to provide inspiration for artificial photosynthetic technologies to meet global energy demand.



1. INTRODUCTION

Emerging solar technology aims to harvest sunlight as an abundant and renewable energy source. Although the flux of sunlight greatly exceeds global power demand, new technology is needed to convert light energy into a storable form.^{1,2} One solution is the splitting of water to dioxygen, protons, and electrons (eq 1).



The protons and electrons produced during this process may be converted into chemical fuels, including H_2 or reduced carbon compounds. Owing to its global abundance, water is an ideal source of reducing equivalents. However, efficient water oxidation remains a barrier to developing molecule-based solar fuels technology.

Nevertheless, global-scale water oxidation already exists as part of the photosynthetic machinery in green plants and cyanobacteria. In photosystem II (PSII), sunlight is used to oxidize water to O_2 and produce reducing equivalents, beginning the electron-transport chain that ultimately results in the synthesis of biomass.^{3,4} Water oxidation occurs at a Mn_4CaO_x cluster within the O_2 -evolving complex (OEC) that is conserved among all known oxygenic photosynthetic species. X-ray crystallography has revealed that the OEC is composed of a “dangling” Mn center connected to a cuboidal Mn_3Ca core (Figure 1).⁵ The mechanistic details are being actively researched in order to implement insights from the natural system into artificial photosynthetic systems for solar fuels.^{3,6} In the cycle proposed by Kok et al.⁷ and shown in Figure 1, O_2

Received: November 19, 2014

Published: March 2, 2015

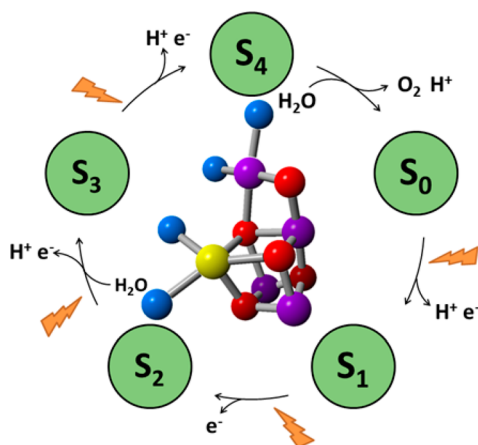


Figure 1. OEC cycles through five light-induced intermediates, releasing O₂ upon formation of the S₄ state. Center: Arrangement of the four Mn (purple), Ca (yellow), and bridging oxides (red) in the OEC. Terminal aqua ligands are shown in blue (PDB ID: 3ARC).

evolution occurs via five intermediates, called S_{*n*} states (*n* = 0–4). The S-state cycle is advanced by light-induced charge separation following the absorption of a photon by the chlorophyll *a* molecules in PSII called P680. Photoexcited P680* transfers an electron to the electron acceptor side of PSII, consisting of a pheophytin, a tightly bound plastoquinone (Q_A), and an exchangeable plastoquinone (Q_B). Meanwhile, oxidized P680 (P680⁺) receives an electron from the OEC, advancing the oxidation state of the Mn cluster. After four successive oxidations, the S₄ state releases O₂ and the OEC is reduced to the S₀ state.

One strategy employed by our group and others for benchmarking calculations or interpreting spectroscopic data on PSII is the study of synthetic model compounds that are structurally or electronically similar to the OEC. Early model chemistry work was focused on the synthesis of high-valent oxomanganese clusters to aid in the interpretation of spectroscopic data and to provide information on the coordination chemistry of manganese in the OEC. The [Mn^{III/IV}₂(bpy)₄(μ-O)₂]³⁺ (bpy = 2,2'-bipyridine) dimer was one of the early complexes widely considered to be a model relevant to the OEC.⁸ A number of di-, tri- and tetranuclear high-valent Mn clusters have been characterized and have provided insight into the structure and function of the OEC. This early work has been extensively reviewed and will not be discussed further.^{9–12}

With the recent atomic-resolution X-ray crystal structures of PSII, the focus of recent manganese model chemistry has shifted to structures more closely related to the OEC. While the exact geometry of the cuboidal cluster is difficult to imitate, manganese complexes of various shapes have been synthesized and characterized.¹³ Despite the number of manganese complexes in the literature, very few of them are functional for water oxidation.¹⁴ In this Account, we summarize our efforts to understand and mimic the function of the OEC by using structurally relevant manganese compounds.

2. A STRUCTURAL AND FUNCTIONAL MODEL OF THE OEC

2.1. Catalytic Water Oxidation

The first reported molecular manganese water-oxidation catalyst was [Mn^{III/IV}₂(terpy)₂(μ-O)₂(OH₂)₂](NO₃)₃, **1**,

where terpy is 2,2',6',2''-terpyridine (Figure 2).¹⁵ This complex features a Mn₂O₂ core that resembles the Mn-di-μ-oxo units

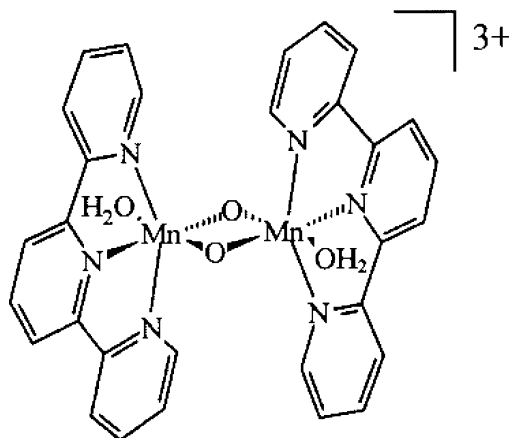


Figure 2. Manganese-terpyridine dimer, **1**.

found in the OEC and in the [Mn^{III/IV}₂(bpy)₄(μ-O)₂]³⁺ dimer that had previously been the leading structural model for the OEC.⁸ However, use of the planar, tridentate terpyridine ligand resulted in coordination of two terminal aqua ligands to manganese and, thus, the formation of exchangeable sites for binding chemical oxidants or substrate water molecules. In the presence of oxo-transfer oxidants such as ClO⁻ or HSO₅⁻ (Oxone), **1** catalyzes O₂ evolution.¹⁵ Initial mechanistic investigations of the O₂-evolving reaction between HSO₅⁻ and **1** revealed that the rate of O₂ evolution saturates at oxidant concentrations above 13 000 equiv with a V_{max} of 2420 mol O₂ (mol **1**)⁻¹ h⁻¹.¹⁶

2.2. Mechanistic Studies

Because HSO₅⁻ acts as an oxo-transfer reagent, the source of the O atoms in the evolved dioxygen is ambiguous and was investigated using isotopic labeling and mass spectrometry. The peroxide bond in HSO₅⁻ does not exchange with water and thus the composition of the O₂ produced in a solution of ¹⁸OH₂ reveals whether the O atoms were derived from the oxidant or water. When the HSO₅⁻ concentration was 100 times the catalyst concentration, 91.9% of the product O₂ was unlabeled ³²O₂, indicating that both O atoms originated from the oxidant.¹⁶ However, when a 20-fold excess of HSO₅⁻ was used, only 49% of the product was unlabeled ³²O₂, with the remaining product having one or both oxygen atoms derived from water. These results suggest that O₂ may be formed by two different pathways.

The formation of dioxygen by two different pathways suggests a branched mechanism, proposed in Figure 3. The saturation of the initial rate is consistent with equilibrium binding of HSO₅⁻ to the manganese dimer followed by rate-determining oxidation.¹⁶ The proposed active species is an electrophilic Mn^{IV}-oxyl that may be nucleophilically attacked by either an additional equivalent of HSO₅⁻ (left branch) or water (right branch). In the case of reaction with water, the complex is reduced by four electrons upon the release of O₂ and must be oxidized by an additional equivalent of HSO₅⁻ to return to the Mn^{III}Mn^{IV} resting state.

Additional studies were performed to characterize the active species and determine the composition of the reaction mixture during catalytic O₂ evolution. The initial Mn^{III}Mn^{IV} state is rapidly consumed after mixing **1** with excess HSO₅⁻ and

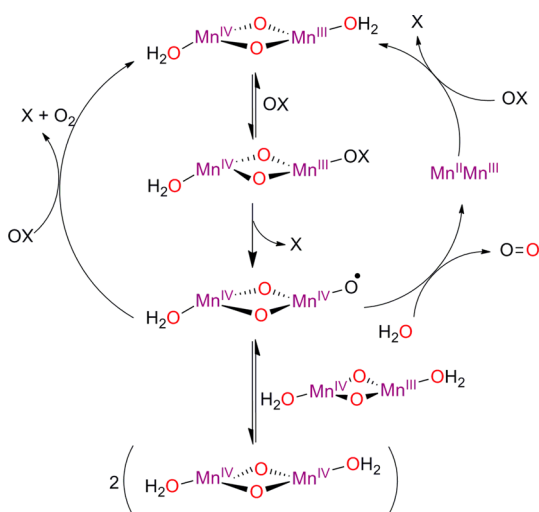


Figure 3. Proposed mechanism for O_2 evolution catalyzed by **1** with an oxygen-atom transfer reagent, OX. Rate-limiting oxidation of the dimer produces a terminal manganese–oxo species that may further react by one of three pathways. Left-hand pathway: attack of OX on the terminal oxo ligand. Right-hand pathway: attack of solvent water on the terminal oxo ligand. Bottom pathway: comproportionation reaction with another equivalent of **1** to form an inactive $\text{Mn}^{\text{IV}}\text{Mn}^{\text{IV}}$ species. The terpyridine ligands are omitted for clarity.

persists as only about 2% of the total Mn concentration during catalysis.¹⁷ The dominant species in solution is the $\text{Mn}^{\text{IV}}\text{Mn}^{\text{IV}}$ complex, characterized by ESI-MS and UV–visible spectroscopy.^{17,18} The rate of O_2 evolution scales linearly with the concentration of the $\text{Mn}^{\text{III}}\text{Mn}^{\text{IV}}$ dimer but is independent of the concentration of the $\text{Mn}^{\text{IV}}\text{Mn}^{\text{IV}}$ species, indicating that the latter species is not part of the catalytic cycle. Stopped-flow kinetic data indicate that the reaction between the $\text{Mn}^{\text{III}}\text{Mn}^{\text{IV}}$ species and HSO_5^- is biphasic at low oxidant concentrations (<5 mM) and monophasic at higher concentrations.¹⁸ This was interpreted to indicate two possible binding sites for HSO_5^- . When HSO_5^- binds to the Mn^{III} site, the complex is slowly oxidized to form a high-valent intermediate, postulated as a terminal $\text{Mn}^{\text{IV}}\text{–oxyl}$ species that reacts quickly with one of three possible partners. The fastest reaction is comproportionation with an equivalent of the $\text{Mn}^{\text{III}}\text{Mn}^{\text{IV}}$ dimer to produce two equivalents of the $\text{Mn}^{\text{IV}}\text{Mn}^{\text{IV}}$ dimer. Kinetic modeling suggests that the rate of this reaction is greater than $2 \times 10^7 \text{ M}^{-1} \text{ s}^{-1}$.¹⁸ Alternatively, the reactive intermediate may form dioxygen through attack by either HSO_5^- or water. The isotope labeling studies described above indicate that reaction with HSO_5^- is faster. This mechanism also explains the relatively high steady-state concentration of the $\text{Mn}^{\text{IV}}\text{Mn}^{\text{IV}}$ species because this reaction will dominate until the concentration of $\text{Mn}^{\text{III}}\text{Mn}^{\text{IV}}$ becomes very low. On the other hand, when HSO_5^- binds to the Mn^{IV} site of the $\text{Mn}^{\text{III}}\text{Mn}^{\text{IV}}$ dimer, oxidation of Mn^{IV} to a formally Mn^{VI} species is not accessible. Instead, the HSO_5^- slowly dissociates from Mn^{IV} to regenerate **1**.¹⁸

2.3. Exchange among Bulk, Terminal, and Bridging Waters

Both bridging and terminal water ligands are known to be present in the OEC,^{5,19,20} and both have been implicated as the substrate-binding sites.³ Water-derived bridging oxo ligands in oxo-bridged Mn complexes serve to stabilize Mn in high oxidation states. However, the labile aqua ligands in **1** play an important role in its water-oxidizing chemistry, as shown by the

lack of activity of analogous coordinatively saturated complexes such as the $[\text{Mn}^{\text{III/IV}}_2(\text{bpy})_4(\mu\text{-O})_2]^{3+}$ dimer.

The exchange between bulk water and substrate waters bound to the OEC has been probed using time-resolved mass spectrometric measurements. The rate of water exchange can place important constraints on the nature of substrate binding and its subsequent oxidation by the OEC. However, knowledge of the exchange properties of water-derived ligands bound to complexes of known structure is necessary in order to interpret these results.

In acetonitrile solution, the bridging oxo ligands of $[(\text{mes-terpy})_2\text{Mn}^{\text{III/IV}}_2(\mu\text{-O})_2(\text{H}_2\text{O})_2](\text{NO}_3)_3$, where mes is a mesityl substituent (Figure 4), exchange completely with the oxygen

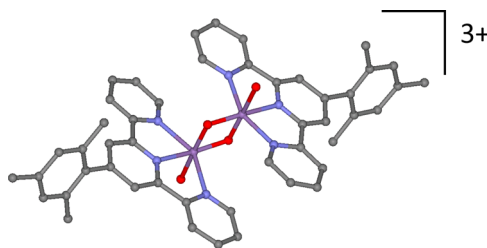


Figure 4. $[(\text{mes-terpy})_2\text{Mn}^{\text{III/IV}}_2(\mu\text{-O})_2(\text{H}_2\text{O})_2](\text{NO}_3)_3$ analogue of **1** used as an acetonitrile-soluble version for μ -oxo exchange studies: carbon (black), oxygen (red), nitrogen (blue), and manganese (purple).

atoms of small amounts of added water within 15 min.²¹ While the specific steps of the exchange mechanism are not entirely clear, both the large, negative entropy of activation and the presence of a $\text{p}K_a$ near 2.5, assigned to the bridging oxo, favor an associative mechanism.²² In this proposal, outlined in Figure 5, exchange is initiated by protonation of the bridging oxo to afford a singly bridged dimer. One metal center is coordinated by a hydroxo ligand formed by the dissociation of the former bridging oxo, while the other metal center binds a bulk water molecule. Exchange occurs when the bridging oxo is reformed, resulting in a statistical incorporation of either the original bridging oxygen or the oxygen from bulk water.²² Each oxo exchanges separately, and the mechanism is symmetrical with respect to the bridge-opened intermediate.

Oxo exchange is very sensitive to the coordination environment and oxidation state of the Mn centers. Complexes in which one of the Mn is a Jahn–Teller distorted Mn^{III} are observed to exchange more quickly than complexes of only Mn^{IV} .²¹ The presence of terminal water ligands may result in intramolecular protonation and, thus, increase the exchange rates compared to coordinatively saturated complexes, such as $[\text{Mn}^{\text{III/IV}}_2(\text{phen})_4(\mu\text{-O})_2](\text{ClO}_4)_3$, which require complete decoordination of the 1,10-phenanthroline (phen) ligand for exchange to occur.²¹

2.4. Water Oxidation in the Presence of Ce^{4+}

In most of the mechanistic studies, a two-electron, O-atom-transfer oxidant was used to drive O_2 evolution. However, one-electron oxidation is more relevant for modeling photosynthetic water oxidation. Ce^{4+} has been widely used as a one-electron oxidant for water oxidation by ruthenium and iridium complexes as well as heterogeneous catalysts due to its high reduction potential (+1.75 V vs NHE, pH 0.9) and single-electron-transfer mechanism.²³

A homogeneous solution of **1** and Ce^{4+} evolves O_2 , demonstrating the ability of **1** to undergo oxidation by single

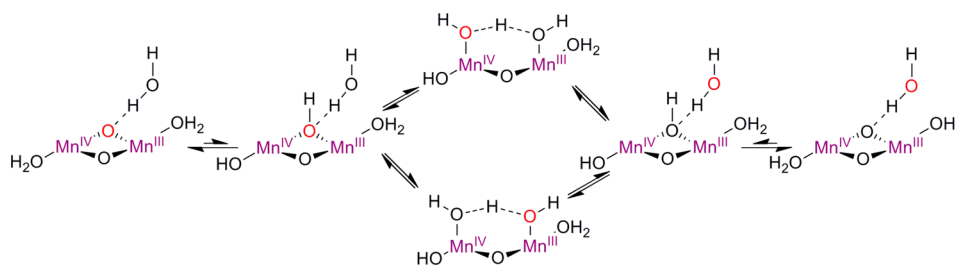


Figure 5. Proposed μ -oxo exchange by an associative mechanism.²²

electron transfer.²⁴ However, the evolved O_2 is substoichiometric, indicating that the active species cannot be regenerated. Part of the cause for catalyst degradation is that the acidic conditions (pH \sim 1) necessary to stabilize Ce^{4+} lead to the disproportionation of **1** to a $Mn^{IV}Mn^{IV}$ dimer and mononuclear Mn^{II} . Below pH 2.5, the $Mn^{IV}Mn^{IV}$ species subsequently dimerizes by μ -oxo bond formation to a less active linear tetrameric Mn^{IV}_4 species $[Mn^{IV}_4O_5(terpy)_4(H_2O)_2]^{6+}$ (Figure 6).²⁵ Additionally, mononuclear Mn^{II} species are formed when

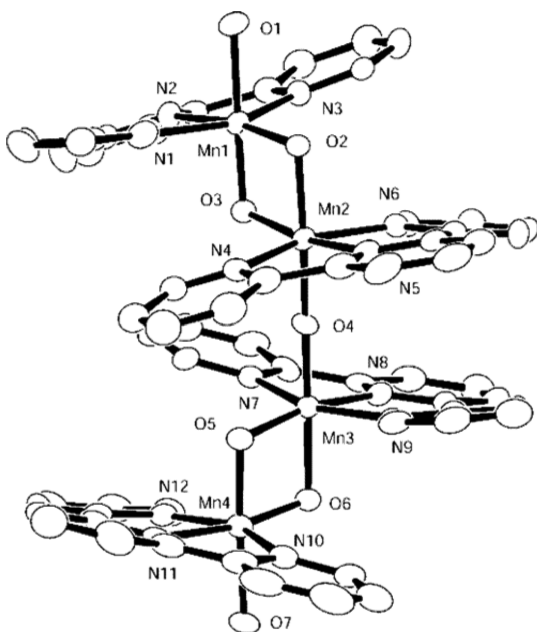


Figure 6. Crystal structure of $[Mn^{IV}_4O_5(terpy)_4(H_2O)_2](ClO_4)_6$, a dimer-of-dimers that forms from disproportionation of **1** under acidic conditions. Reproduced ref 25. Copyright 2004 American Chemical Society.

the catalyst is reduced during water oxidation. While HSO_5^- is able to oxidize these Mn^{II} species, leading to manganese dimerization and reformation of the active catalyst, Ce^{4+} is unable to do so, precluding catalytic turnover. Interestingly, $[Mn^{IV}_4O_5(terpy)_4(H_2O)_2]^{6+}$ (Figure 6) has been suggested to evolve O_2 electrochemically by oxidation of the Mn^{IV}_4 species to a formally $Mn^{IV}_3Mn^V$ species that reacts with water to release O_2 .²⁶

Yagi and Narita have noted that catalytic O_2 evolution can be observed when **1** is immobilized in Kaolin clay and Ce^{4+} is used as oxidant.²⁷ Over 7 days, 13.5 mol of O_2 per mole of **1** was observed in the presence of Ce^{4+} , suggesting that immobilization of the complex may mitigate the dissociation of Mn centers when the oxo-bridges break, allowing for reassembly of the catalytic species. Similarly, sustained water oxidation is

observed when **1** is isolated in a metal–organic framework and Oxone is used as oxidant.²⁸

2.5. Toward Artificial Photosynthesis

Proceeding from the characterization of a functional mimic for the OEC of PSII, we desired to connect the catalyst to other functional components that mimic the light-harvesting and electron-accepting components of PSII. In a water-oxidizing photoanode based on dye-sensitized mesoporous metal oxide semiconductors such as TiO_2 , a photosensitizer initiates charge separation by absorbing a photon, much like P680 in PSII.²⁹ The excited state of the synthetic photosensitizer is poised to transfer an electron to the conduction band of the semiconductor, mimicking the acceptor side of PSII. The hole remaining on the photosensitizer oxidizes the water-oxidation catalyst, mimicking the donor side of PSII.

As a first step, the catalyst was immobilized on a TiO_2 surface without a photosensitizer to determine whether electrons could be transferred from the catalyst to the semiconductor.³⁰ While the exact mode of deposition is difficult to characterize, a change in the ^{55}Mn hyperfine coupling in the EPR spectrum of the adsorbed complex and quantum mechanical calculations suggested that an oxo-bridge forms between a surface Ti^{IV} and the manganese complex, replacing one of the terminal water-binding sites.³⁰ Chemically driven water oxidation was observed in the presence of Ce^{4+} when the complex was immobilized on nanocrystalline P25 TiO_2 .³⁰

In order to add a light-harvesting component to the immobilized catalyst system, we designed a chromophoric surface linker, **L**, with an acetylacetonate functional group for attachment to TiO_2 and a terpyridine group to coordinate manganese.³¹ The Mn–terpy dimer catalyst could be assembled on the surface by coordination of Mn^{2+} to the surface-bound ligand and subsequent oxidation by permanganate (Figure 7), confirmed by the observation of the characteristic 16-line EPR spectrum.³¹

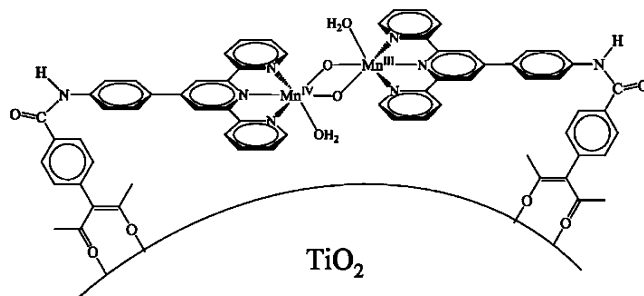


Figure 7. Proposed configuration of the Mn–terpy dimer immobilized on a TiO_2 surface by a chromophoric linker, **L**, with an acetylacetonate anchoring group. Reproduced from ref 31. Copyright 2010 American Chemical Society.

When the $\text{TiO}_2\text{-L-Mn}$ catalyst system was illuminated with >425 nm light at low temperature, the EPR signal of the $\text{Mn}^{\text{III}}\text{Mn}^{\text{IV}}$ dimer was attenuated by about 19%.³¹ This was interpreted to indicate reversible photooxidation of $\text{Mn}^{\text{III}}\text{Mn}^{\text{IV}}$ to EPR-silent $\text{Mn}^{\text{IV}}\text{Mn}^{\text{IV}}$ via electron injection into the TiO_2 conduction band from the photoexcited chromophore and oxidation of the catalyst by the subsequently formed organic cation radical. However, no further photooxidation or photocatalytic activity was observed.

3. INSIGHT INTO PHOTOSYNTHETIC WATER OXIDATION

The reactivity and properties of **1** and its analogues have been compared to those of the Mn_4CaO_x cluster of the OEC, providing corroborating evidence for a number of known processes in the natural system as well as additional insight into the more intricate mechanistic complexities. Here, we provide a summary of this comparison, highlighting what the model complexes can teach us about the OEC and how the OEC can help us to design better models.

3.1. Substrate Binding to the OEC

In both the OEC (Figure 1) and **1** (Figure 2), the Mn ions have two types of water-derived oxygen ligands: terminal and bridging. The terminal aqua ligands have been shown to be substrates for **1**. The OEC has nine water-derived ligands: five bridging oxo/hydroxo and four terminal aqua/hydroxo ligands. Currently, the locations of the binding sites and the binding modes of the two substrate waters remain a subject of debate. Studies of model systems have aided in the interpretation of the relative time scales of μ -oxo exchange, O_2 evolution, and valence delocalization of PSII in order to evaluate the reasonableness of proposed mechanisms.

The bridging μ -O and terminal water sites of **1** are analogous to those of the OEC, allowing for a general comparison. For the model complexes, terminal aqua ligands are found to exchange rapidly (<10 s) for both Mn^{III} and Mn^{IV} , whereas μ -O ligands exchange much more slowly for mixed-valence complexes containing Mn^{III} and Mn^{IV} and not at all for $\text{Mn}^{\text{IV}}\text{Mn}^{\text{IV}}$ complexes.²¹ These observations can be compared to the substrate exchange kinetics that have been measured for the OEC in each of the $\text{S}_0\text{-S}_3$ states.³² Biphasic kinetics are observed for the OEC in the S_2 and S_3 states, attributed to different rates of exchange of the two substrate waters, each on a millisecond time scale. On the basis of the much slower rates of μ -O exchange in model complexes than the rates of substrate exchange in the OEC, our studies of oxo-bridged manganese complexes provided evidence that substrates in the OEC are bound as terminal ligands.^{21,22,33} However, more recent work^{34,35} has revealed that one of the μ -O ligands in the OEC exchanges rapidly in the S_1 state (<15 s), and this has spurred proposals invoking a μ -O species as one of the substrates in the OEC. An investigation of factors affecting μ -O exchange rates in model complexes revealed that μ -O exchange is initiated by protonation of the bridging oxo.²² Because the pK_a of μ -O ligands decreases dramatically when the Mn ions are oxidized from $\text{Mn}^{\text{III}}\text{Mn}^{\text{IV}}$ to $\text{Mn}^{\text{IV}}\text{Mn}^{\text{IV}}$, the μ -O ligands should not be easily protonated in $\text{Mn}^{\text{IV}}\text{Mn}^{\text{IV}}$ complexes, consistent with the observation that μ -O ligands do not exchange in $\text{Mn}^{\text{IV}}\text{Mn}^{\text{IV}}$ model complexes.²¹ Because the S_3 state of the OEC has four Mn^{IV} ions, μ -O exchange should not occur in this state. However, substrate water exchange is observed on a millisecond time scale. Therefore, we interpret the substrate

exchange rates measured in the OEC as terminal aqua or hydroxo ligand exchange rates. The activation energies measured for substrate exchange in the OEC are in the range of 10 to 20 kcal mol⁻¹.³⁶ Our simulation of terminal ligand exchange rates on **1** is consistent with these numbers¹⁸ as well as with calculated rates of terminal aqua and hydroxo ligand exchange on Mn^{IV} dimers and monomers³⁷ and the S_1/S_2 states of the OEC.³⁸

The time scale for conversion of the S_3 state to the S_0 state in the Kok cycle, concomitant with O_2 evolution, has been measured to be ~ 1 ms.³⁹ During water oxidation, one Mn center is likely to be more oxidized than the adjacent Mn centers and act as the active site for O–O bond formation. On the basis of its proximity to tyrosine Z, the redox intermediate that oxidizes the OEC, the dangling Mn center,⁴⁰ which has two terminal aqua ligands in the 1.9 Å X-ray crystal structure,⁵ may be the Mn center oxidized in the S_4 state. In order to facilitate an oxidative process at this center, valence delocalization in the OEC should be slower than the O–O bond-formation step. Biphasic kinetics in the oxidation of **1** by HSO_5^- have led us to propose that the rate of intramolecular electron transfer between the Mn centers in **1** is 5 s⁻¹ or less ($t_{1/2} \geq 140$ ms).¹⁸ We expect the rate of valence delocalization in the OEC to be similar, suggesting that it may be possible to localize the oxidizing power on a single Mn ion within the OEC for a longer time than the time required for the O–O bond-forming reaction.

Together, these studies indicate that the substrate waters are likely bound terminally to the metal centers in the OEC during photosynthetic water oxidation. Progressive oxidation of the Mn ions in the OEC during the S-state transitions could then lead to a high-valent manganese species that is localized on the dangling Mn in order to activate a substrate water molecule for O–O bond formation.

3.2. Mn–Oxyl as the Water-Oxidizing Species

A high-valent manganese with terminally bound oxygen has been implicated as the water-oxidizing species in photosynthetic water oxidation as well as in complex **1**. For the OEC, successive photoinduced oxidations of the Mn_4CaO_x cluster occur during the Kok cycle, with the dangling Mn proposed to form the active high-valent species for O–O bond formation as discussed above.⁴¹ This putative high-valent manganese has been described as $\text{Mn}^{\text{V}}=\text{O}$,^{3,42–45} although DFT calculations provide evidence for a $\text{Mn}^{\text{IV}}\text{-O}^\bullet$ species where the active electrophilic species is delocalized over both Mn and oxygen.^{41,46}

For complex **1**, the formation of the active water-oxidizing species is hypothesized to occur by a two-electron oxidation of the $\text{Mn}^{\text{III}}\text{Mn}^{\text{IV}}$ complex, as shown in Figure 3.¹⁸ The results of isotope incorporation from bulk water into the evolved O_2 are consistent with either a $\text{Mn}^{\text{V}}=\text{O}$ or $\text{Mn}^{\text{IV}}\text{-O}^\bullet$ intermediate being the water-oxidizing species in the model system, whereas quantum calculations have indicated that a $\text{Mn}^{\text{IV}}\text{-oxyl}$ intermediate is involved in the O–O bond-forming reaction.^{16,17,47} However, the transient nature of both the S_4 state in the OEC and the O_2 -evolving intermediate of complex **1** has precluded its direct experimental observation.

3.3. Advantages of a Protein Environment

In the case of photosynthetic water oxidation, a number of properties of the OEC are optimized by the protein structure. The slowest step for turnover of the OEC is 1–2 ms, which gives the OEC the capacity to evolve oxygen at a rate of up to

500–1000 s⁻¹. However, the rate-limiting step for PSII turnover is quinone reduction and exchange on the electron acceptor side so that the maximum observed rate of oxygen evolution by PSII is about 40 per second with a turnover number (TON) of 600 000.^{14,48} Both the turnover frequency (TOF) and TON are dramatically better than those achieved to date for model manganese complexes.¹⁴

Along with O₂ evolution, water oxidation produces protons that must be shuttled away from the OEC to avoid pH changes. Protein side chains are capable of controlling the local pH around the active site via proton-shuttle pathways.⁴⁹ Without a controlled local environment around the catalyst, degradation can occur. This was shown to be the case for complex **1**, where low pH can cause disproportionation and oligomerization as discussed above.^{25,26} Efficient proton transport by the protein to remove protons generated during the water-oxidation process is, thus, an integral part of the stability of the OEC during continuous catalytic turnover.

Protein amino acid residues can also interact directly with the Mn₄CaO_x cluster in the OEC to help form and stabilize it, particularly while in lower valent states. It is known that the apo-PSII protein, without the OEC cluster, is capable of generating an active OEC under illumination in the presence of soluble OEC precursors.⁵⁰ After the OEC forms with successive oxidations by the PSII tyrosine radical, and with the help of the protein matrix as a scaffold, it is stable to catalytic turnover. Complex **1** mimics this assembly process during its synthesis, using the terpyridine ligand to bind a soluble manganese source and HSO₅⁻ as the oxidizing equivalents to form the active dimeric species. As described above, clay²⁷ or a metal–organic framework,²⁸ acting as a heterogeneous surface for catalyst interaction, promotes stability of the molecular intermediates much like a protein scaffold.

Interaction of the protein with the OEC is also a way to control the highly oxidizing active site. As can be expected, catalysis is based on available oxidizable substrates, with water being one of many possibilities. The oxidizing power of the OEC needs to be targeted to its specific substrate, avoiding oxidative damage to PSII or other proteins in the photosynthetic cell. This is achieved both by a rigid framework to prevent reaction of the reactive high-valent Mn–oxo intermediates with protein residues and also by the existence of well-defined channels for entry of water and exit of protons produced by the oxidation of water.³ For **1**, lack of control in solution allows for dimers to interact, comproportionating to form the inactive Mn^{IV}Mn^{IV} dimer or other higher nuclearity species.¹⁷

3.4. Necessity of a Tetranuclear Cluster

The properties of the dimeric complex **1** underscore the necessity of a tetranuclear system for tuning the redox potentials and maintaining the stability of the cluster beyond the influence of the protein scaffold. Current evidence suggests that the OEC cycles between the formal oxidation states of Mn^{III}₃Mn^{IV} in the S₀ state and Mn^{IV}₃Mn^V in the S₄ state. Notably, this range avoids labile Mn^{II} at any point in the Kok cycle. As described above, the formation of Mn^{II} is proposed to be one of the likely decomposition pathways for **1**. In addition, a greater nuclearity of the cluster than two could lower the pK_a of the oxo bridges in the lower-valent states of the cluster, thereby lessening the potential for hydrolysis and resulting in greater acid stability of the OEC.

The higher ratio of oxo bridges per manganese in the OEC (Figure 1) compared to that in **1** (Figure 2) also has significant effects on the manganese electrochemical potentials. In **1**, only the oxidation of Mn^{III}Mn^{IV} to Mn^{IV}Mn^{IV} is observed in the electrochemical window between +0.9 and +1.7 V vs NHE.^{15,51} By contrast, all four S-state transitions in the tetranuclear OEC occur within a narrow range of electrochemical potentials, and all are under the potential of P680^{•+} (~1.26 V vs NHE) that functions as the primary oxidant of the OEC. Similarly, trinuclear manganese model complexes have been shown to stabilize higher oxidation states compared to dinuclear analogues.^{52,53} Oxo-bridges are electron-donating, so the higher average ratio of oxo-bridges to manganese in the OEC and its higher-order structure allow for greater leveling of the electrochemical potentials for the four Mn atoms during oxidation. Both higher nuclearity and greater oxo-bridging in the OEC provide electronic and structural stabilization of the electronically coupled redox-active cluster.¹¹

4. SUMMARY

The manganese–terpyridine dimer described here is the first example of a molecular multiple-turnover O₂-evolution catalyst using manganese. The structure of **1** resembles the oxo-bridged active site of PSII, and the O–O bond-forming reaction is suggested to proceed through similar Mn^{IV}–oxyl intermediates in both systems. Comparisons between the OEC and **1** highlight the importance of encapsulation of reactive intermediates as well as redox leveling in multielectron processes. Because **1** is a functional model of the OEC, it is useful for benchmarking studies of future functional analogues. Studies of this complex exemplify the dialogue between biomimetic chemistry and the natural system. The model complexes provide insight into the complex mechanism of PSII, whereas discrepancies between the behavior of the model and natural systems offer directions for improvement of the synthetic systems toward applications in solar energy conversion.

AUTHOR INFORMATION

Corresponding Author

*Phone: 203-432-5202; Fax: 203-432-6144; E-mail: gary.brudvig@yale.edu.

Present Addresses

†(K.J.Y.) Centre College, Danville, Kentucky 40422, United States.

‡(R.T.) Biocon, Bangalore 560 100, India.

Notes

The authors declare no competing financial interest.

Biographies

Karin J. Young received a B.A. from The University of Tulsa in 2008 and a Ph.D. from Yale University in 2013 with Gary W. Brudvig. She is currently Assistant Professor of Chemistry at Centre College.

Bradley J. Brennan received a B.S. from Drake University in Des Moines, Iowa, in 2005 and a Ph.D. from Arizona State University in 2012 with Devens Gust. He is currently an Associate Research Scientist at the Energy Sciences Institute at Yale University.

Ranitendranath Tagore received a B.S. from Presidency College, Calcutta, in 1999, a M.S. from the Indian Institute of Technology, Mumbai, in 2001, and a Ph.D. under the joint guidance of Robert Crabtree and Gary Brudvig at Yale University in 2006. Following

postdoctoral study in the laboratories of Richard Holm and Alan Saghatelian at Harvard University, he is currently employed as a Scientific Manager at Biocon Research Limited, Bangalore, India.

Gary W. Brudvig received a B.S. in 1976 from the University of Minnesota and a Ph.D. in 1981 from Caltech working with Sunney Chan and was a Miller Postdoctoral Fellow with Ken Sauer at the University of California, Berkeley, from 1980 to 1982. He has been on the faculty at Yale University since 1982, where he currently is the Benjamin Silliman Professor of Chemistry, Professor of Molecular Biophysics and Biochemistry, and Director of the Yale Energy Sciences Institute.

ACKNOWLEDGMENTS

Current support from the U.S. Department of Energy, Division of Chemical Sciences, Geosciences, and Biosciences, Office of Basic Energy Sciences, Office of Science is gratefully acknowledged for our studies of photosystem II (DE-FG02-535 05ER15646) and oxomanganese complexes (DE-FG02-07ER15909). Earlier work was supported by the National Institutes of Health (grant GM32715).

REFERENCES

- (1) Lewis, N. S.; Nocera, D. G. Powering the planet: chemical challenges in solar energy utilization. *Proc. Natl. Acad. Sci. U.S.A.* **2006**, *103*, 15729–15735.
- (2) Young, K. J.; Martini, L. A.; Milot, R. L.; Snoeberger, R. C., III; Batista, V. S.; Schmuttenmaer, C. A.; Crabtree, R. H.; Brudvig, G. W. Light-driven water oxidation for solar fuels. *Coord. Chem. Rev.* **2012**, *256*, 2503–2520.
- (3) McEvoy, J. P.; Brudvig, G. W. Water-splitting chemistry of photosystem II. *Chem. Rev.* **2006**, *106*, 4455–4483.
- (4) Yano, J.; Yachandra, V. Mn_4Ca cluster in photosynthesis: where and how water is oxidized to dioxygen. *Chem. Rev.* **2014**, *114*, 4175–4205.
- (5) Umena, Y.; Kawakami, K.; Shen, J.-R.; Kamiya, N. Crystal structure of oxygen-evolving photosystem II at a resolution of 1.9 Å. *Nature* **2011**, *473*, 55–60.
- (6) Cox, N.; Retegan, M.; Neese, F.; Pantazis, D. A.; Boussac, A.; Lubitz, W. Electronic structure of the oxygen-evolving complex in photosystem II prior to O–O bond formation. *Science* **2014**, *345*, 804–808.
- (7) Kok, B.; Forbush, B.; McGloin, M. Cooperation of charges in photosynthetic oxygen evolution. I. A linear four step mechanism. *Photochem. Photobiol.* **1970**, *11*, 457–475.
- (8) Cooper, S. R.; Calvin, M. Mixed valence interactions in di- μ -oxo bridged manganese complexes. *J. Am. Chem. Soc.* **1977**, *99*, 6623–6630.
- (9) Christou, G. Manganese carboxylate chemistry and its biological relevance. *Acc. Chem. Res.* **1989**, *22*, 328–335.
- (10) Brudvig, G. W.; Thorp, H. H.; Crabtree, R. H. Probing the mechanism of water oxidation in photosystem II. *Acc. Chem. Res.* **1991**, *24*, 311–316.
- (11) Manchanda, R.; Brudvig, G. W.; Crabtree, R. H. High-valent oxomanganese clusters—structural and mechanistic work relevant to the oxygen-evolving center in photosystem II. *Coord. Chem. Rev.* **1995**, *144*, 1–38.
- (12) Mukhopadhyay, S.; Mandal, S. K.; Bhaduri, S.; Armstrong, W. H. Manganese clusters with relevance to photosystem II. *Chem. Rev.* **2004**, *104*, 3981–4026.
- (13) Tsui, E. Y.; Kanady, J. S.; Agapie, T. Synthetic cluster models of biological and heterogeneous manganese catalysts for O_2 evolution. *Inorg. Chem.* **2013**, *52*, 13833–13848.
- (14) Cady, C. W.; Crabtree, R. H.; Brudvig, G. W. Functional models for the oxygen-evolving complex of photosystem II. *Coord. Chem. Rev.* **2008**, *252*, 444–455.
- (15) Limburg, J.; Vrettos, J. S.; Liable-Sands, L. M.; Rheingold, A. L.; Crabtree, R. H.; Brudvig, G. W. A functional model for O–O bond formation by the O_2 -evolving complex in photosystem II. *Science* **1999**, *283*, 1524–1527.
- (16) Limburg, J.; Vrettos, J. S.; Chen, H.; de Paula, J. C.; Crabtree, R. H.; Brudvig, G. W. Characterization of the O_2 -evolving reaction catalyzed by [(terpy)(H_2O) $Mn^{III}(O)_2Mn^{IV}(OH)_2(terpy)](NO_3)_3$ (terpy = 2,2':6,2''-terpyridine). *J. Am. Chem. Soc.* **2001**, *123*, 423–430.
- (17) Chen, H.; Tagore, R.; Olack, G.; Vrettos, J. S.; Weng, T.-C.; Penner-Hahn, J.; Crabtree, R. H.; Brudvig, G. W. Speciation of the catalytic oxygen evolution system: $[Mn^{III/IV}_2(\mu-O)_2(terpy)_2(H_2O)_2](NO_3)_3 + HSO_5^-$. *Inorg. Chem.* **2007**, *46*, 34–43.
- (18) Tagore, R.; Crabtree, R. H.; Brudvig, G. W. Oxygen evolution catalysis by a dimanganese complex and its relation to photosynthetic water oxidation. *Inorg. Chem.* **2008**, *47*, 1815–1823.
- (19) Ferreira, K. N.; Iverson, T. M.; Maghlaoui, K.; Barber, J.; Iwata, S. Architecture of the photosynthetic oxygen-evolving center. *Science* **2004**, *303*, 1831–1838.
- (20) Loll, B.; Kern, J.; Saenger, W.; Zouni, A.; Biesiadka, J. Towards complete cofactor arrangement in the 3.0 Å resolution structure of photosystem II. *Nature* **2005**, *438*, 1040–1044.
- (21) Tagore, R.; Chen, H.; Crabtree, R. H.; Brudvig, G. W. Determination of μ -oxo exchange rates in di- μ -O di-manganese complexes by electrospray ionization mass spectrometry. *J. Am. Chem. Soc.* **2006**, *128*, 9457–9465.
- (22) Tagore, R.; Crabtree, R. H.; Brudvig, G. W. Distinct mechanisms of bridging-oxo exchange in di- μ -O dimanganese complexes with and without water-binding sites: implications for water binding in the O_2 -evolving complex of photosystem II. *Inorg. Chem.* **2007**, *46*, 2193–2203.
- (23) Parent, A. R.; Crabtree, R. H.; Brudvig, G. W. Comparison of primary oxidants for water-oxidation catalysis. *Chem. Soc. Rev.* **2013**, *42*, 2247.
- (24) Tagore, R.; Chen, H.; Zhang, H.; Crabtree, R. H.; Brudvig, G. W. Homogeneous water oxidation by a di- μ -oxo dimanganese complex in the presence of Ce^{4+} . *Inorg. Chim. Acta* **2007**, *360*, 2983–2989.
- (25) Chen, H.; Faller, J. W.; Crabtree, R. H.; Brudvig, G. W. Dimer-of-dimers model for the oxygen-evolving complex of photosystem II. Synthesis and properties of $[Mn^{IV}_4O_5(terpy)_4(H_2O)_2](ClO_4)_6$. *J. Am. Chem. Soc.* **2004**, *126*, 7345–7349.
- (26) Gao, Y.; Crabtree, R. H.; Brudvig, G. W. Water oxidation catalyzed by the tetranuclear Mn complex $[Mn^{IV}_4O_5(terpy)_4(H_2O)_2](ClO_4)_6$. *Inorg. Chem.* **2012**, *51*, 4043–4050.
- (27) Yagi, M.; Narita, K. Catalytic O_2 evolution from water induced by adsorption of $[(OH_2)(terpy)Mn(\mu-O)_2Mn(terpy)(OH_2)]^{3+}$ complex onto clay compounds. *J. Am. Chem. Soc.* **2004**, *126*, 8084–8085.
- (28) Nepal, B.; Das, S. Sustained water oxidation by a catalyst cage-isolated in a metal–organic framework. *Angew. Chem., Int. Ed.* **2013**, *52*, 7224–7227.
- (29) McConnell, I.; Li, G.; Brudvig, G. W. Energy conversion in natural and artificial photosynthesis. *Chem. Biol.* **2010**, *17*, 434–447.
- (30) Li, G.; Sproviero, E. M.; Snoeberger, R. C., III; Iguchi, N.; Blakemore, J. D.; Crabtree, R. H.; Brudvig, G. W.; Batista, V. S. Deposition of an oxomanganese water oxidation catalyst on TiO_2 nanoparticles: computational modeling, assembly and characterization. *Energy Environ. Sci.* **2009**, *2*, 230.
- (31) Li, G.; Sproviero, E. M.; McNamara, W. R.; Snoeberger, R. C.; Crabtree, R. H.; Brudvig, G. W.; Batista, V. S. Reversible visible-light photooxidation of an oxomanganese water-oxidation catalyst covalently anchored to TiO_2 nanoparticles. *J. Phys. Chem. B* **2010**, *114*, 14214–14222.
- (32) Hillier, W.; Wydrzynski, T. ^{18}O -Water exchange in photosystem II: substrate binding and intermediates of the water splitting cycle. *Coord. Chem. Rev.* **2008**, *252*, 306–317.
- (33) Brudvig, G. W. Water oxidation chemistry of photosystem II. *Philos. Trans. R. Soc., B* **2008**, *363*, 1211–1219.
- (34) McConnell, I. L.; Grigoryants, V. M.; Scholes, C. P.; Myers, W. K.; Chen, P.-Y.; Whittaker, J. W.; Brudvig, G. W. EPR–ENDOR characterization of (^{17}O , 1H , 2H) water in manganese catalase and its

relevance to the oxygen-evolving complex of photosystem II. *J. Am. Chem. Soc.* **2011**, *134*, 1504–1512.

(35) Rapatskiy, L.; Cox, N.; Savitsky, A.; Ames, W. M.; Sander, J.; Nowaczyk, M. M.; Rögner, M.; Boussac, A.; Neese, F.; Messinger, J.; Lubitz, W. Detection of the water-binding sites of the oxygen-evolving complex of photosystem II using W-band ^{17}O electron–electron double resonance-detected NMR spectroscopy. *J. Am. Chem. Soc.* **2012**, *134*, 16619–16634.

(36) Hillier, W.; Wydrzynski, T. Substrate water interactions within the photosystem II oxygen evolving complex. *Phys. Chem. Chem. Phys.* **2004**, *6*, 4882–4889.

(37) Lundberg, M.; Blomberg, M. R. A.; Siegbahn, P. E. M. Modeling water exchange on monomeric and dimeric Mn centers. *Theor. Chem. Acc.* **2003**, *110*, 130–143.

(38) Sproviero, E. M.; Shinopoulos, K.; Gascón, J. A.; McEvoy, J. P.; Brudvig, G. W.; Batista, V. S. QM/MM computational studies of substrate water binding to the oxygen-evolving centre of photosystem II. *Philos. Trans. R. Soc., B* **2008**, *363*, 1149–1156.

(39) Haumann, M.; Liebisch, P.; Müller, C.; Barra, M.; Grabolle, M.; Dau, H. Photosynthetic O_2 formation tracked by time-resolved X-ray experiments. *Science* **2005**, *310*, 1019–1021.

(40) Peloquin, J. M.; Campbell, K. A.; Randall, D. W.; Evanchik, M. A.; Pecoraro, V. L.; Armstrong, W. H.; Britt, R. D. ^{55}Mn ENDOR of the S_2 -state multiline EPR signal of photosystem II: implications on the structure of the tetranuclear Mn cluster. *J. Am. Chem. Soc.* **2000**, *122*, 10926–10942.

(41) Sproviero, E. M.; Gascoñ, J. A.; McEvoy, J. P.; Brudvig, G. W.; Batista, V. S. Quantum mechanics/molecular mechanics study of the catalytic cycle of water splitting in photosystem II. *J. Am. Chem. Soc.* **2008**, *130*, 3428–3442.

(42) Pecoraro, V. L.; Baldwin, M. J.; Caudle, M. T.; Hsieh, W. Y.; Law, N. A. A proposal for water oxidation in photosystem II. *Pure Appl. Chem.* **1998**, *70*, 925–929.

(43) McEvoy, J. P.; Brudvig, G. W. Structure-based mechanism of photosynthetic water oxidation. *Phys. Chem. Chem. Phys.* **2004**, *6*, 4754–4763.

(44) Isobe, H.; Shoji, M.; Koizumi, K.; Kitagawa, Y.; Yamanaka, S.; Kuramitsu, S.; Yamaguchi, K. Electronic and spin structures of manganese clusters in the photosynthesis II system. *Polyhedron* **2005**, *24*, 2767–2777.

(45) McEvoy, J. P.; Gascon, J. A.; Batista, V. S.; Brudvig, G. W. The mechanism of photosynthetic water splitting. *Photochem. Photobiol. Sci.* **2005**, *4*, 940–949.

(46) Siegbahn, P. E. M.; Crabtree, R. H. Manganese oxyl radical intermediates and O–O bond formation in photosynthetic oxygen evolution and a proposed role for the calcium cofactor in photosystem II. *J. Am. Chem. Soc.* **1999**, *121*, 117–127.

(47) Lundberg, M.; Blomberg, M. R. A.; Siegbahn, P. E. M. Oxyl radical required for O–O bond formation in synthetic Mn-catalyst. *Inorg. Chem.* **2004**, *43*, 264–274.

(48) Berthold, D. A.; Babcock, G. T.; Yocum, C. F. A highly resolved, oxygen-evolving photosystem II preparation from spinach thylakoid membranes: EPR and electron-transport properties. *FEBS Lett.* **1981**, *134*, 231–234.

(49) Ishikita, H.; Saenger, W.; Loll, B.; Biesiadka, J.; Knapp, E.-W. Energetics of a possible proton exit pathway for water oxidation in photosystem II. *Biochemistry* **2006**, *45*, 2063–2071.

(50) Miller, A. F.; Brudvig, G. W. Manganese and calcium requirements for reconstitution of oxygen-evolution activity in manganese-depleted photosystem II membranes. *Biochemistry* **1989**, *28*, 8181–8190.

(51) Cady, C. W.; Shinopoulos, K. E.; Crabtree, R. H.; Brudvig, G. W. $[(\text{H}_2\text{O})(\text{terpy})\text{Mn}([\mu\text{-O})_2\text{Mn}(\text{terpy})(\text{OH}_2)](\text{NO}_3)_3$ (terpy = 2,2':6,2''-terpyridine) and its relevance to the oxygen-evolving complex of photosystem II examined through pH dependent cyclic voltammetry. *Dalton Trans.* **2010**, *39*, 3985–3989.

(52) Sarneski, J. E.; Thorp, H. H.; Brudvig, G. W.; Crabtree, R. H.; Schulte, G. K. Assembly of high-valent oxomanganese clusters in

aqueous solution. Redox equilibrium of water-stable $\text{Mn}_3\text{O}_4^{4+}$ and $\text{Mn}_2\text{O}_2^{3+}$ complexes. *J. Am. Chem. Soc.* **1990**, *112*, 7255–7260.

(53) Pal, S.; Chan, M. K.; Armstrong, W. H. Ground spin state variability in manganese oxo aggregates. Demonstration of an $S = 3/2$ ground state for $[\text{Mn}_3\text{O}_4(\text{OH})(\text{bpea})_3](\text{ClO}_4)_3$. *J. Am. Chem. Soc.* **1992**, *114*, 6398–6406.